

In Vitro Bioactivity and Antibacterial Activity of Zn and Sr Containing Glass Ionomer Cement Prepared by a Quick Alkali-Mediated Sol-Gel Method

Taha M Tiama^{1*}, Nagy Abd El Sameea², Khairy M Tohamy³ and Islam E Soliman⁴

¹Research Assistant, Knowledge Center, Faculty of Pharmacy, Misr University for Science and Technology, 6th of October, Egypt

²Professor and Head of Dental Material Department, Faculty of Dentistry, Modern University for Technology and Information, Egypt

³Professor, Biophysics Department, Faculty of Science, Al-Azhar University, Nasr City, Cairo, Egypt

⁴Lecturer, Biophysics Department, Faculty of Science, Al-Azhar University, Nasr City, Cairo, Egypt

*Corresponding Author: Taha M Tiama, Research Assistant, Knowledge Center, Faculty of Pharmacy, Misr University for Science and Technology, 6th of October, Egypt.

Received: November 03, 2017; Published: December 07, 2017

Abstract

Glass-ionomer cements were synthesized through a quick alkali mediated sol-gel method which has composition SiO_2 , Al_2O_3 , Na_2O , CaO , P_2O_5 , F- with substitute ZnO by SrO additive. Adding ZnO and SrO effect on the bioactivity of cured ionomer cement was examined in simulated body fluid (SBF). The ideal powder: liquid (P: L) ratio determined to prepare the experimental GICs was equal to 1:1.5. The chemical process which use to allow the development of glass powder at 400°C which is the aim of the present paper. We characterized the powders by thermal analysis (TG/DSC), X-ray diffraction analysis (XRD), Fourier transforms infrared (FTIR) and Antibacterial test. The results showed that ZnO and SrO adding to glass ionomer cement block sites of the apatite nucleation led to retardation the apatite formation, high antimicrobial effect of samples against *Escherichia coli*, *Staphylococcus Staph* and also showed increase hardness by adding zinc contents.

Keywords: GICs; Sol-Gel; Bioactivity; PPA; Antibacterial; Hardness

Introduction

Conventional glass-ionomer cements (GIC) consisting of a base usually an ion-leachable, calcium aluminum fluorosilicate glass powder – that is combined with polyacrylic acid (PAA) or its copolymers were first described by Wilson and kent in 1971 [1]. GIC was only from the early 1980s on that their physical properties were improved, thus making these materials more applicable and popular [2]. Many of the features have contributed to their wide acceptance, which include compatibility with life, good adhesion to dentin, the ability to handle and release fluoride, minimal shrinkage on the development and resistance to degradation similar to that of dentin [3].

GICs are materials made of calcium or strontium alumino fluorosilicate glass powder (base) combined with a water soluble polymer (acid). Kent called such materials “glass ionomer” cements, and that name has become part of the dental vernacular [4]. GICs components, when mixed together, undergo a setting reaction involving neutralization of the acid groups by the powdered solid glass base. Treatment reactions occur in two phases designated as gelation and maturation. These two cement processing phases generate the structure of GIC, a composite of cross-linked PAA reinforced with the reacted glass particles [5]. Without reducing the physical properties of hardened cement, large amounts of fluoride ions are released during this reaction.

The acid reacts with the basic SrO and ZnO to form a cross-linked metal polyacrylate salt containing residual SrO and ZnO particles. These Polyalkenoate cements set at body temperature without undergoing any shrinkage polymerization without significant development of heat [6]. The focus is on the development of glass ionomer cement due to their excellent biocompatibility in the mouth, with no significant adverse reactions reported in over 20 years of use [7].

In human subjects body growth and development is strictly dependent on Zinc. The nervous, reproductive and immune systems are particularly influenced by Zinc deficiency. Zinc plays an active role in bone metabolism and tooth formation. Zinc increases the alkaline phosphatase activity in the bone without changing the enzyme synthesis; thus the bone mineralization is inhibited [8,9].

Sr - containing bioactive glasses in SiO₂-CaO-SrO system by sol-gel method. The results pertaining to *in vitro* bioactivity analysis of the as developed glasses exhibited their strong potential towards osteoporosis treatment, dental applications and in bone tissue regeneration as well in bone remodeling. Further, substituting strontium ions in place of calcium, magnesium and to other alkaline earth cations showed good results in terms of bioactivity which sometimes claimed to be most challenging and also witnessed some phenomenal exchange of ideas and outcome which kindled the research of Sr-doped glasses with respect to the bone tissue engineering [10]. Calcium fluoro-alumina-silicate glasses may be regarded as the basic type from which GICs are derived. These systems are prepared by melting method at temperatures ranging from 1200 to 1550oC, depending on the composition. In this process, fluorine is lost from the melting. This fluorine loss is uncontrolled and results in variable composition between batches [11]. Instead, soft chemistry has been used for synthesis of glasses because this route yields more homogeneous materials using less processing temperatures than the conventional melt method. In addition, the sol-gel process has the potential to yield glasses which cannot be otherwise prepared by the conventional melting method due to their high melting points [12]. Considerable efforts have been made to improve the properties of GICs using other types of glass powders derived from calcium fluoro-alumino-silicate systems with new components. The aim of this study, Zn containing glass ionomer cement was prepared by sol-gel method, with the purpose to analyses its bioactivity, hardness, antibacterial properties and the influence of Zn, Sr and both of them on the deposition of HA on its surface.

Materials and Methods

Tetraethyl orthosilicate (TEOS), calcium nitrate tetrahydrate Ca(NO₃)₂·H₂O, sodium nitrate NaNO₃, Aluminum nitrate Al(NO₃)₃·9H₂O Zinc nitrate hexahydrate Zn(NO₃)₂·6H₂O, Strontium nitrate Sr(NO₃)₂, Ammonium fluoride NH₄F as source to fluorine and triethyl phosphate (TEP) (≥ 98%) were purchased from Fluka (Buchs, Switzerland). Ammonia solution, 33%, and nitric acid, 68%, were purchased from Merck, USA. Both nitric acid and ammonia solutions were diluted to 2M (mol) using distilled water.

Sol-gel synthesis of Zinc-doped glass ionomer

Glass containing 0, 4, 6, 8 and 10 wt% of ZnO samples was synthesized through a quick alkali-mediated sol-gel technique [13]. ZnO was added to the glass compositions at the expense of SrO. Table 1 shows the nominal compositions and codes of the prepared bioactive glass, we make three solutions A), TEOS, distilled water and 2M nitric acid (as a hydrolysis catalyst), were successively mixed in ethanol and the mixture was left to react for 30 min under continuous magnetic stirring for the acid hydrolysis of TEOS. Then appropriate amounts of series reagents were added in the following sequence: (TEP), Ca(NO₃)₂·H₂O, NaNO₃, NH₄F and Zn(NO₃)₂·6H₂O, allowing 30 min for each reagent to react completely. B) Sr(NO₃)₂ were mixed in the presence of distal water, C) Al(NO₃)₃·9H₂O is mixed in distal water, then solutions B and C are added on A by dropping for 30 minutes under continuous magnetic stirring. After the final addition, mixing was of all reagents continued for 60 minutes to complete hydrolysis. Ammonia solution of 2M concentration (a gelation catalyst) was dropped into the mixture. The mixture was then agitated with glass rod (like as mechanical stirrer) to prevent the formation of a bulk gel. Finally, each prepared gel was left to dry at 100 - 120°C for 2 days and sintered at 400°C for 2hr thermal oven.

Glass	Glass base							Additives
	SiO ₂	Al ₂ O ₃	P ₂ O ₅	CaO	Na ₂ O	F ⁻	SrO	ZnO
Zn ₀ , Sr ₀	45	15	5	15	10	10	---	---
Zn ₀	45	15	5	10	5	10	10	---
Zn ₄	45	15	5	10	5	10	6	4
Zn ₆	45	15	5	10	5	10	4	6
Zn ₈	45	15	5	10	5	10	2	8
Zn ₁₀	45	15	5	10	5	10	0	10

Table 1: Shows different additive of ZnO on the: SiO₂-Al₂O₃-P₂O₅-CaO-Na₂O-SrO-F⁻.

Cement preparation

The powder glass was passed through a sieve with a mesh opening of 45 µm, and then was used to produce the cement. The power of GICs were prepared at room temperature by mixing the powder prepared by the sol - gel process with aqueous solutions 45 - 50% (m/m) of poly (acrylic acid) – PAA– MW 230,000. The specimens were made using a powder: liquid (P: L) ratio of 1:1.5. This P: L ratio (m/m) [14].

Characterization

Differential calorimetric analyses (DSC), and thermogravimetric analyses (TGA) were performed for the dried gels using a computerized SETARAM labsys™ TG-DSC thermal analysis system. Scans were performed in the atmosphere, and in a temperature range of 50 - 1000°C, at a rate of 10°C min⁻¹. The materials were analyzed using aluminum oxide powder as a reference. The phase analysis of the samples was examined by X-ray diffractometer; model BRUKERaxs using Ni-filtered CuKα irradiation at 40 kV and 25 mA. The infrared spectra of the prepared glass were obtained using Fourier transform infrared spectrophotometer (FT-IR) (Model 580, Perkin-Elmer). Each sample used for infrared spectroscopic analysis was prepared according to KBr technique.

In-vitro assays in SBF

In-vitro assays were performed in a simulated body fluid (SBF), proposed by Kokubo., *et al* [15]. The SBF solution has a composition and concentration similar to those inorganic parts of human plasma. In the soaking process, each 0.3g powder was soaked into 200 ml SBF contained in a polyethylene bottle. We covered these bottles with a tight lid and placed in thermodynamic incubator at 37°C for different time periods (control, 1, 4, 8 and 16 days). After being soaked, the discs were rinsed with deionized water and acetone and dried at room temperature.

Micro-hardness Test

Surface Micro-hardness of the specimens was determined using Digital Display Vickers Micro-hardness Tester (Model HVS-50, Laizhou Huayin Testing Instrument Co., Ltd. China) with a Vickers diamond indenter and a 20X objective lens. A load of 200g was applied to the surface of the specimens for 10 seconds. Three indentations, which were equally placed over a circle and not closer than 1 mm to the adja-

cent indentations or to the margin of the specimens, were made on the surface of each specimen. The diagonal length of the indentations was measured by being built in scaled microscope and Vickers values were converted into micro-hardness values.

The Vickers indenter usually produces a geometrically similar indentation at all test forces (Figure 1). For isotropic materials, the two diagonals of a Vickers indentation meanwhile are equal in size. Vickers hardness number, HV, is an expression of hardness obtained by dividing the force applied to a Vickers indenter by the surface area of the permanent impression made by the indenter. In practice, test loads are in grams-force and indentation diagonals are in micrometers.

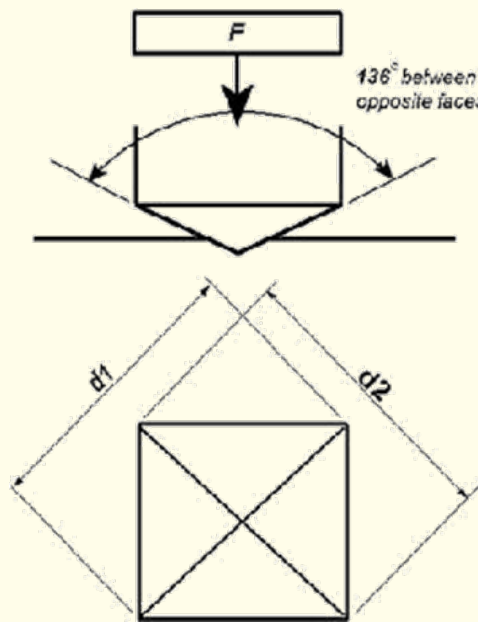


Figure 1: Vickers micro-hardness geometry.

Micro-hardness was obtained using the following equation:

$$HV = 1.854 P/d^2$$

Where, HV is Vickers hardness in kg/mm², P is the load in kg, and d is the length of the diagonals in mm.

Hardness improvement of dental cement using zinc oxide in SI units (GPa), Vickers hardness is determined as follows:

$$HV = 0.0018544 \times P_1/d_1^2$$

Where, P₁ = force, N, and d₁ = length of the long diagonal of the indentation, mm

Indentations were done on three different points of each pellet and the average hardness obtained was considered to be the hardness number on the Vickers scale.

Antibacterial tests

Antibacterial Property Was examined by mixing the same physiologic solution was used for bacteria. 500 µL of containing bacteria solution were in contact in plate at room temperature for 15, 30 minutes, 1 and 2h, After each sampling time, EC X-GLUC agar for *E. coil* and AZIDE MALTOSE agar (KF) for *S. Staph* were added to sample plates. The plates were aerobically incubated 48h at 37°C for *E. coil*, *S. Staph*. The number of the colonies was counted.

Results and Discussion

Thermal analysis

Thermogravimetric analysis (TGA) and differential scanning calorimetric (DSC), analysis curves for sample (Zn₄) are shown in figure 2, 3. The TGA curves of all samples showed three main stages of weight losses as the heating process proceeded from room temperature up to 800°C. Those weight losses appeared at the temperature intervals of 30 - 160, 160 - 224, 224 - 305, and 305 - 700°C for all samples. The first weight loss was attributed to the removal of water which appears as (humidity and physically adsorbed water) from the surface and any the residual alcohol in the pores of the dried gel [16]. This stage was reflected in the DCS curves of sample (Zn₄) as the first large endothermic peak centered at about 160°C [16], as shown in figure 2. The second weight loss was reflected in the exothermic peaks centered around at 224°C on the DSC curve of sample (Zn₄), which is most likely due to first crystallization temperature for CaF₂ phase separation.

The third weight loss occurred from the end of the second drop in mass around at 284°C until around at 551°C leading to an apparent weight loss about 13.45% of the total weight loss. This weight loss is due to second crystallization temperature for calcium aluminium silicate ($\text{Ca}_3\text{Al}_6\text{Si}_2\text{O}_{16}$), as confirmed by the corresponding second exothermic peak at 700°C in the DSC trace [17].

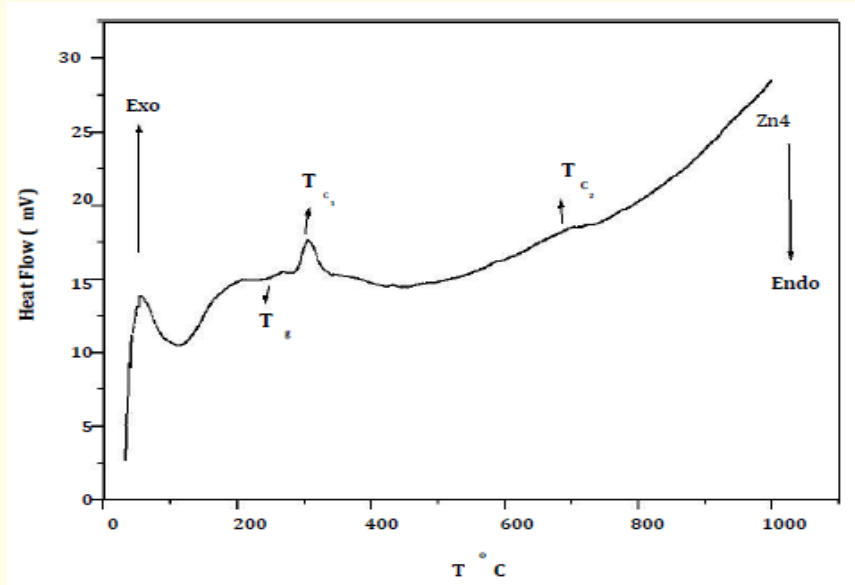


Figure 2: DSC curves of sol-gel glass after drying for all samples at 80°C and 120°C for 2 days.

X-ray diffraction Analysis

The powder prepared at 400°C by the sol - gel process was analyzed by X-ray powder diffraction (XRD) to identify the crystal phases. In figure 3, four peaks at 2 θ values of 28.27°, 47.09°, 55.7° and 68.66° were observed. This crystalline phase corresponds to the standard JCPDS file no. (88-2301), which refers to the presence of fluorite (CaF_2) phase. The crystallization of CaF_2 occurs because Ca^{2+} and F- ions are relatively mobile in network [11].

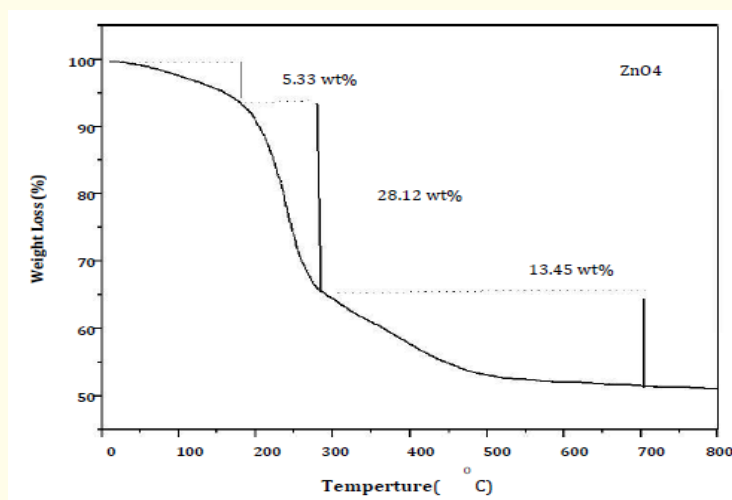


Figure 3: TGA curve of sol-gel glass for Zn4 sample.

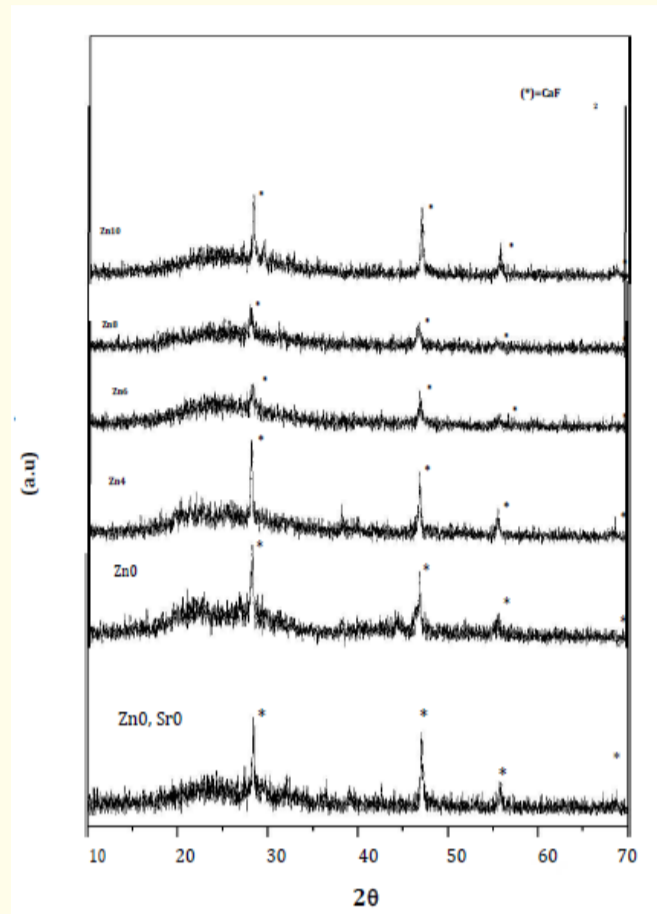


Figure 4: XRD Pattern of all sol-gel GIC samples soaking in SBF.

The XRD analysis results of annealing gel glass ionomer cement samples after soaking in SBF for Zn₀, Zn₄ and Zn₁₀ at 400°C are shown in figure 5. after soaking in SBF for 16 days, there are two phases formed on the GICs surface. The first phase is poor-crystallized HA layer exhibit as small peaks which overlapping with CaF₂ peaks. In addition, the second phase is the well-crystallized phase calcium Oxide (CaO).

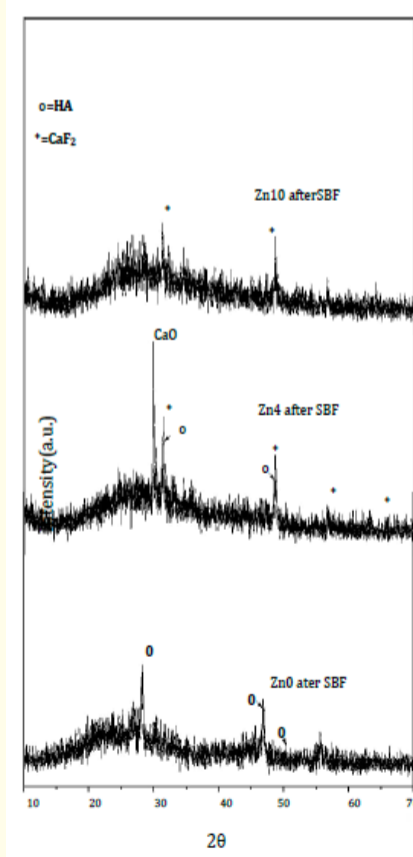


Figure 5: XRD Pattern of all sol-gel GIC samples after soaking in SBF.

Generally, the increase in the intensity and decrease in the width of the apatite peaks of all samples in SBF depends on amount of ZnO contents. Therefore, the presence of Zn²⁺ ions in the GICs composition causes inhibition or retardation of calcium phosphate precipitation layer by adsorbing onto the top and block sites of the calcium phosphate nucleation [18].

FTIR analysis

The FTIR spectra of the cement samples (cured for 24h) were used to characterize their curing reactions and chemical structure of silicate network for all samples as shown in figure 6. The observed bands of all samples are listed in table 2. For all samples before adding PAA, the bands in the range of 1000 - 1300 cm⁻¹ correspond to the Si-O-Si asymmetric stretching vibration whereas the band located at ~ 440 - 540 cm⁻¹ corresponds to the vibrational mode of the bending of Si-O-Si [19]. The two absorption bands located at ~ 670-740 cm⁻¹ corresponds to Si-O symmetric stretch of bridging oxygen (BO) between tetrahedron chains.

Band range cm ⁻¹	Zn ₀	Zn ₄	Zn ₆	Zn ₈	Zn ₁₀
Si-O-Si (b) 540 - 440	440	441	440	442	443
Si-O (s) 670 - 740	...	680	731,740	687	690
Si-O-Si (s) 1000 - 1300	111 3	1095	1089	1085	1078
P-O (b) 550 - 640	607	570	566	562	555
C-O (s) 1300 - 1500	146 1	1462	1520	1460	1464
H-O-H 1630 - 1650	164 4	1632	1650	1640	149
H-O-H (s) 3350 - 3600	335 0	3438	3453	3432	3430
NO ₃ ⁻ 1385	138 5	1384	1386	1382	1385

Table 2: Assignments of Infra-red absorption bands of Zn₀, Zn₄, Zn₆, Zn₈ and Zn₁₀

On the other hand, FTIR spectra of glass after adding with PAA (GICs) are shown in figure 6. The general features observed were a progressive conversion of acid -COOH groups to salt -COO- groups as metal salts were formed. On neutralization of organic acid the main characteristic is loss of bands around 1250 and 1710 cm-1 assigned to C-O and C=O stretch of poly(acrylic acid) in the FTIR spectra. Loss of these bands is due to formation of polyacrylate salts [20,21].

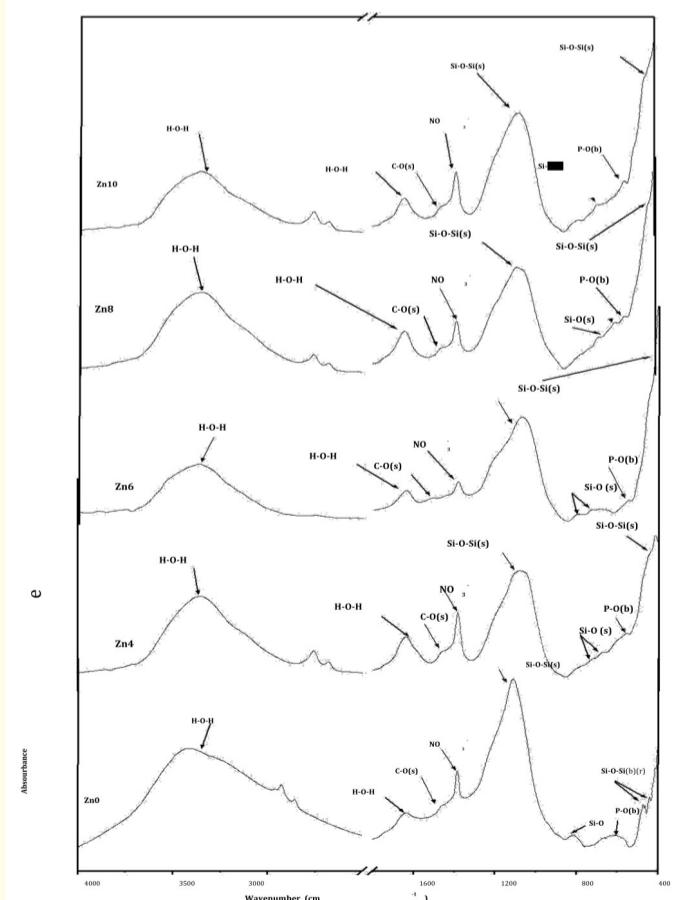


Figure 6: FTIR spectra of Zn₀, Zn₄, Zn₆, Zn₈ and Zn₁₀ sol-gel glass.

As can be seen in figure 7 The bands observed around 1700 cm⁻¹ were substituted progressively and other bands can be observed in the spectra. These bands around 1460 and 1640cm⁻¹ (after 24h) could be assigned to symmetric and asymmetric COO⁻ stretch of aluminum polyacrylate salt and the bands around 1380cm⁻¹ assigned to symmetric COO⁻ stretch of calcium poly acrylate. These data confirm that the reaction between the particles of the powder and poly(acrylic acid) solution was completed within 24h after that cement had been prepared [14].

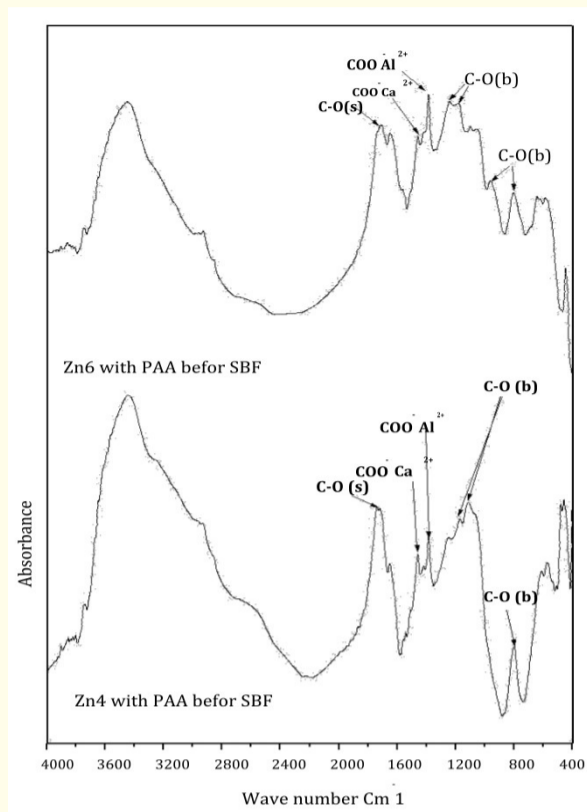


Figure 7: FTIR spectra of Zn₄ and Zn₆ sol-gel GICs after mixing with poly (acrylic acid) before SBF.

Figure 8 Shows FTIR absorption spectra of glass ionomer cement samples after soaking in SBF for 16 days. These spectra of GICs sample after SBF immersion showed either a single peak or a split peak approximately at 610 cm⁻¹ and 530 cm⁻¹ which attributed to P-O bending vibration [22]. This is the most characteristic region for apatite and other phosphates, and it corresponds to P-O bonding vibrations in a PO₃⁴⁻ tetrahedron and indicates the presence of crystalline calcium phosphates including apatite phase (HA), but with small amount.

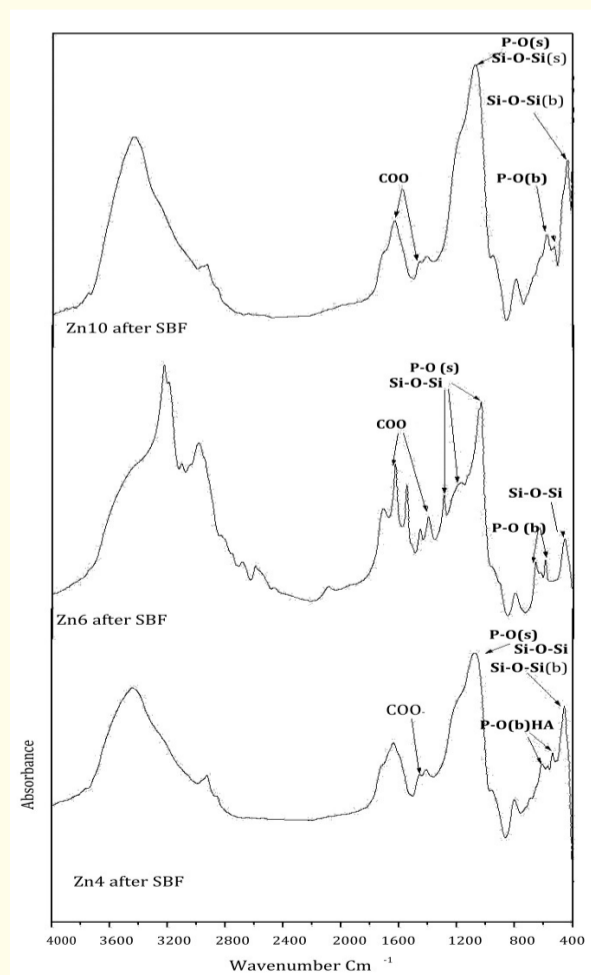


Figure 8: FTIR spectra of Zn₄, Zn₆ and Zn₁₀ sol-gel GICs after mixing with poly (acrylic acid) and soaking in SBF.

This delay in apatite layer formation is due to two reasons: the first is the presence of Zn²⁺ ions which blocking the nucleation site of apatite phase.

The second is the presence of PAA, which plays a role in the change of pH value in SBF solution [23]. Consequently, it is assumed that PAA does not inhibit the formation of the apatite nucleation sites, but does inhibit the formation of apatite and/or crystal growth on these nucleation sites [24]. Therefore, the apatite formation on the surface of the glass ionomer cement may be inhibited by the adsorption of PAA and release of Zn ions to compete with Ca ions in SBF solution.

Micro-hardness Test

From figure 9, it can be observed that hardness of the GICs increases with the increasing amount of ZnO annealed at temperature 400°C added into it. This might be due to higher annealing temperature used in the production of Glass ionomer cement powder which creates a coarser crystal size. Mechanical properties of a material vary with the increase in particle size. The largest Vickers hardness number observed is 57.16 g/lm², corresponding to the 10 % of 400°C ZnO that was added.

Sample	Load (g)	Dwell time(s)	Hardness (HV)	Mean hardness (HV)
Zn ₄	200g	10	43.53092	42.92
			40.61065	
			44.75212	
Zn ₆	200g	10	49.30487	50.47
			52.0639	
			50.05419	
Zn ₁₀	200g	10	55.57424	57.16
			52.27021	
			63.6466	

Table 3: Change in hardness of the GICs with the addition of ZnO at 400°C.

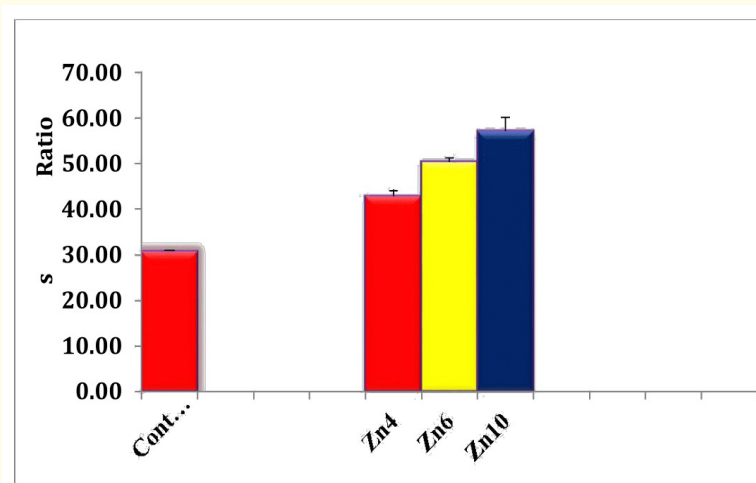


Figure 9: Means (±standard Error) (Vickers) of microhardness values.

This due to, the ionic radius of Zn²⁺ (0.74Å) is smaller than the ionic radius of Sr²⁺ (1.18Å). So, the addition of ZnO has a smaller disrupting effect on the structure and hence it will strengthen the network JC Knowles., *et al.* (2001) [25]. This result was in agreement with that of Boyd D., *et al.* [26] who worked on a SrO – CaO – ZnO – SiO₂ glass ionomer composition and that of Abou Neel EA., *et al.* [27] who worked on Sr-doped phosphate glasses. The replacement may cause a significant increase in GIC hardness due to increasing the network disorder caused by smaller ionic radius of Zn compared with Sr.

Antibacterial test of (GICs)

Plates (A, B) illustrate the test results for the glass ionomer cement containing zinc respectively. The diameters of the halo zone for the antibacterial materials are demonstrated in table 4. The diameters of haloes of inhibition were measured using calipers. Disc diameters were measured at the same point and the size of inhibition zones was calculated as follows: size of inhibition zone (mm) = (diameter of zone of inhibition–diameter of disc) × 1/2, as shown in figure 9.

Sample Name	Size of inhibition zone area (cm)	
	<i>Escherichia coli</i>	<i>Staphylococcus Staph</i>
Zn ₀ Sr ₀	0.30 cm	0.35 cm
Zn ₀	0.35 cm	0.70 cm
Zn ₄	0.40 cm	0.75 cm
Zn ₆	0.44 cm	0.80 cm
Zn ₈	0.50 cm	0.85 cm
Zn ₁₀	0.67 cm	1.0 cm

Table 4: The diameter of the halo zone which made by the antibacterial materials.

The antibacterial assay revealed that samples Zn₀, Zn₄, Zn₆, Zn₈ and Zn₁₀ had an antibacterial effect against *Staphylococcus Staph* and *E. coli* as shown in figure 10. There is a clear difference between the inhibitory effects of the cements on *E. coli* and *S. Staph* viscosus. Figure 10 illustrate the inhibition zones around the GICs disks in the agar plate after 48h. The diameters of inhibition zones formed around all GICs disks were about 0.35 - 67 cm to *E. coli* and 0.7 - 1 cm to *S. Staph*.

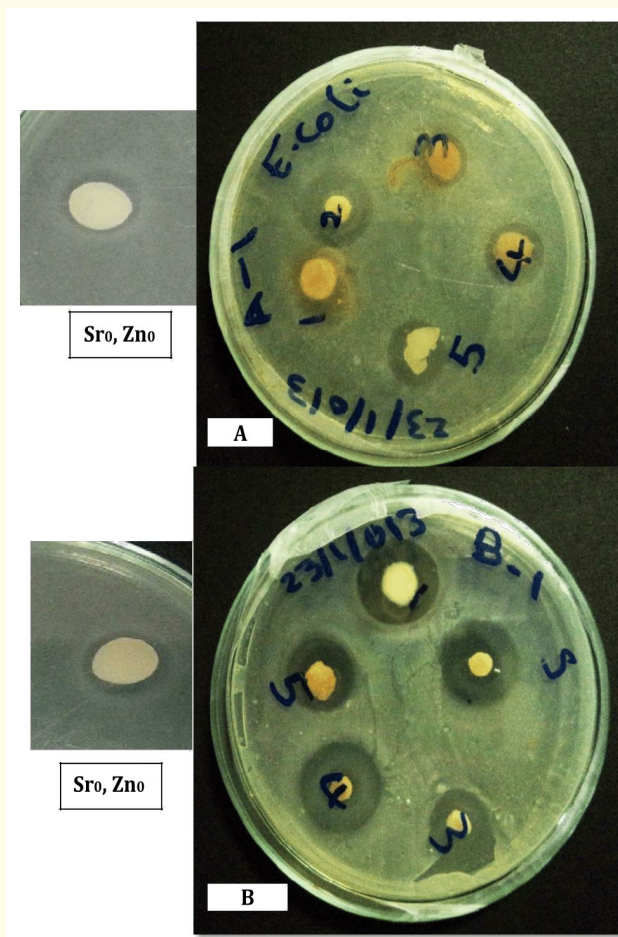


Figure 10: The antibacterial efficiency of antibacterial glass ionomer cement containing zinc in the test microorganisms (A: *Escherichia coli* B: *Staphylococcus Staph*).

The antibacterial action of the Zinc-doped GICs was attributed to the leaching out of Zn²⁺ ions from the glass matrix. Phan T-N., *et al.* [28] studied the antibacterial effect of Zn²⁺ ions and suggested that zinc inhibits multiple activities in the bacterial cell, such as glycolysis, transmembrane proton translocation and acid tolerance, it has been shown to exhibit an antibacterial effect at considerably lower concentrations than many antimicrobial agents [29]. Nevertheless, the cements without Sr and with different Zn content exhibited different inhibition of both bacterial species.

Conclusions

ZnO Containing SiO₂, Al₂O₃, Na₂O, CaO, P₂O₅, F- glass-ionomer cement were successfully prepared by quick alkali mediated sol-gel method. The present results indicate that, with the partial substitution of ZnO for SrO in glass composition and then mixed with PPA, the formation of apatite-like layer is delayed, asserting that, not all GICs surfaces are equally active for nucleation of apatite crystals. Thus, the apatite formation on the surface of the GICs may be inhibited by the reduction of PAA and release of Zn ions to contest with Ca ions in SBF solution. The antibacterial test revealed that all glass ionomer cements samples had an antibacterial effect against to different type of bacteria, which could confirm their ability to treat bone infection and has been avowed as an antibacterial agent. Finally, glass ionomer cements should be characterized as three properties, the first is formation of a small apatite layer to biocompatible with the Facial and jaw bones, and the second is antibacterial effect to set one's face against Oral bacteria and the third is high hardness by increase ZnO, which is the most important feature.

Bibliography

1. Wilson AD and Kent BE. "The glass-ionomer cement, a new translucent dental filling material". *Journal of Applied Chemistry and Biotechnology* 21.11 (1971): 313.
2. Abdalla AI and Garcia-Godoy F. "Bond strengths of resin-modified glass ionomers and polyacid-modified resin composites to dentin". *American Journal of Dentistry* 10.6 (1997): 291-294.
3. Fruits TJ., *et al.* "Uses and properties of current glass ionomer cements: a review". *General Dentistry* 44.5 (1996): 410-418.
4. Wilson AD and McLean JW. Quintessence Publishing Co (1888): 14.
5. Pires RA., *et al.* "Structural and spatially resolved studies on the hardening of a commercial resin-modified glass-ionomer cement". *Journal of Materials Science: Materials in Medicine* 18.5 (2007): 787-796.
6. Hse KY., *et al.* "Resin Ionomer materials for children: A review". *Australian Dental Journal* 44.1 (1999): 1-11.
7. Mount GJ. "Clinical performance of glass-ionomers". *Biomaterials* 19.6 (1998): 573-579.
8. Underwood EJ. "Trace Element in Human and Animal Nutrition, 4th edition". Academic Press, London (1997): 196.
9. Yamaguchi M., *et al.* "Action of zinc on bone metabolism in rats. Increases in alkaline phosphatase activity and DNA content". *Biochemical Pharmacology* 35.5 (1987): 773-777.
10. Lao J., *et al.* "New strontium-based bioactive glasses: physicochemical reactivity and delivering capability of biologically active dissolution products". *Journal of Materials Chemistry* 19 (2009): 2940-2949.
11. Wood D and Hill R. "Glass ceramic approach to controlling the properties of a glass-ionomer bone cement". *Biomaterials* 12.2 (1991): 164-170.
12. Taira M and Yamaki M. "Preparation of SiO₂-Al₂O₃ glass powders by the sol-gel process for dental applications". *Journal of Materials Science: Materials in Medicine* 6.4 (1995): 197-200.
13. El-Gohary MI., *et al.* "Influence of composition on the in-vitro bioactivity of bioglass prepared by a quick alkali-mediated sol-gel method". *Nature and Science* 11.3 (2013): 33.

14. Bertolini MJ., *et al.* "Determination of the properties of an experimental glass polyalkenoate cement prepared from niobium silicate powder containing fluoride". *Dental Materials* 24.1 (2008): 124-128.
15. Kokubo T and Takadama H. "How useful is SBF in predicting in vivo bone bioactivity?" *Biomaterials* 27.15 (2006): 2907-2915.
16. Oki A., *et al.* "Preparation and in vitro bioactivity of zinc containing sol-gel-derived bioglass materials". *Journal of Biomedical Materials Research* 69.2 (2004): 216-221.
17. Jonesa JR., *et al.* "Optimising bioactive glass scaffolds for bone tissue engineering". *Biomaterials* 27.7 (2006): 964-973.
18. Hesaraki S., *et al.* "Physico-chemical and in vitro biological evaluation of strontium/calcium silicophosphate glass". *Journal of Materials Science: Materials in Medicine* 21.2 (2010): 695-705.
19. Aguiar H., *et al.* "Structural study of sol-gel silicate glasses by IR and Raman spectroscopies". *Journal of Non-Crystalline Solids* 355.8 (2009): 475-480.
20. Young AM. "FTIR investigation of polymerisation and polyacid neutralisation kinetics in resin-modified glass-ionomer dental cements". *Biomaterials* 23.15 (2002): 3289-3295.
21. Young AM., *et al.* "Use of Raman spectroscopy in the characterisation of the acid-base reaction in glass-ionomer cements". *Biomaterials* 21.19 (2000): 1971-1979.
22. Vidueau V and Dupius J. "Phosphates and biomaterials". *European Journal of Solid State and Inorganic Chemistry* 28 (1991): 303-343.
23. Kamitakahara M., *et al.* "Effect of polyacrylic acid on the apatite formation of a bioactive ceramic in a simulated body fluid: fundamental examination of the possibility of obtaining bioactive glass-ionomer cements for orthopaedic use". *Biomaterials* 22.23 (2001): 3191-3196.
24. Amjad Z. "Performance of polymeric additives as HA crystal growth inhibitors". *Phosphorus Research Bulletin* 5 (1995): 1-12.
25. Knowles JC., *et al.* "Investigation of the solubility and ion release in the glass system K₂O-Na₂O-CaO-P₂O₅". *Biomaterials* 22.23 (2001): 3091-3096.
26. Boyd D., *et al.* "The role of Sr²⁺ on the structure and reactivity of SrO-CaO-ZnO-SiO₂ ionomer glasses". *Journal of Materials Science: Materials in Medicine* 19.2 (2008): 953-957.
27. Abou Neel EA., *et al.* "Structure and properties of strontium-doped phosphate-based glasses". *Journal of the Royal Society Interface* 6.34 (2009): 435-446.
28. Phan T-N., *et al.* "Physiologic actions of zinc related to inhibition of acid and alkali production by oral streptococci in suspensions and biofilms". *Oral Microbiology and Immunology* 19.1 (2002): 31-38.
29. Brading MG., *et al.* "Anti-microbial efficacy and mode of action studies on a new zinc/ Triclosan formulation". *International Dental Journal* 53 (2003): 363-370.

Volume 16 Issue 4 December 2017

© All rights reserved by Taha M Tiama., et al.